Supplementary Material

S1.1 Risk perception and Risk aversion

The DUE functions in Equations 1, 2, and 3 are a function of risk aversion (Equation S1), which is assumed to be constant based on Gandelman, Nestor (2015).

$$U(x) = \frac{x^{1-\sigma}}{1-\sigma} \qquad \text{(S1)}$$

The risk perception parameter β is used to capture bounded rationality. Following Ruig et al. (2022) and Haer et al. (2020), we define β over time, as in Equation S2:

$$\beta_t = c * 1.6^{-d*t} + 0.01 \qquad \text{(S2)}$$

S1.2. Annexures

[FAO Annexure for crop data]

[Farm distribution from Lowder et al. (2016)]

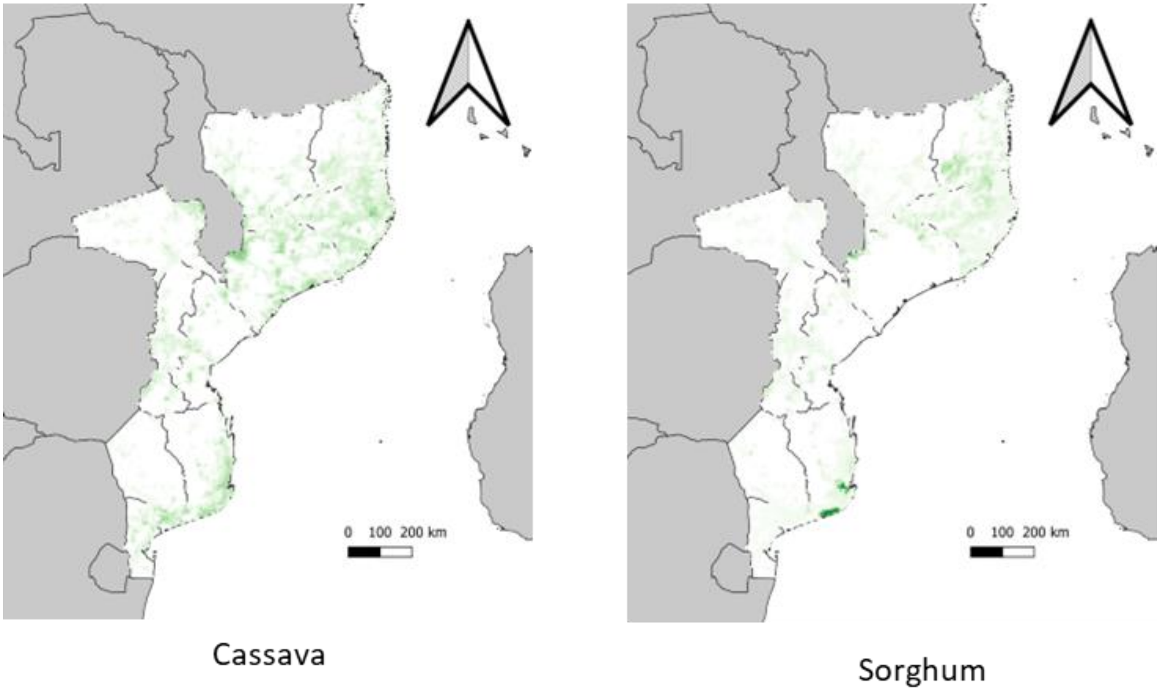

Figure S1 Spatial distribution of crops in Mozambique in 2015. Downscaled and resampled from the GAEZ v4 portal (https://gaez.fao.org/)

S1.3. Model scenarios

We modelled the input scenarios for different climate scenarios based on RCP-SSP-coupled scenarios. We used RCP4.5 coupled to SSP2 and RCP8.5 coupled to SSP5 use a baseline scenario of no SLR under SSP2. IIASA projections for SSP2 (coupled with RCP 4.5) and SSP5 (coupled with RCP 8.5) scenarios are used for population growth. In this procedure, we adjust the total population of the country to the population projected under the medium population growth scenario of the World Population Prospects (United Nations 2019). Since we do not know future fertility rates, we adjust the natural population change *r* (Kummu M et al., 2013) for each department using a factor *a* (equation below) and optimize it at each time step using the Nelder-Mead optimization algorithm (Gao, F. & Han, L. 2010). In addition, the income growth captured by GDP per capita (Figure S2 b) has a direct impact on the cost parameters (*F*, Equation S4), such as property value, adaptation cost, seed cost and farmer's selling price in the market, according to Equation S4, where r_t is the growth rate at time *t*.

$$\boldsymbol{r_i} = \begin{Bmatrix} \boldsymbol{r_i * (1 + a)\ if\ r_i \geq 0} \\ \boldsymbol{r_i * (1 - a)\ if\ \ r_i < 0} \end{Bmatrix} \qquad \text{(S3)}$$

$$\boldsymbol{F(t) = \ r_t * F(t - 1)} \qquad \text{(S4)}$$

Scenario	Unit	2010	2015	2020	2025	2030	2035	2040	2045	2050	2055	2060	2065	2070	2075	2080	2085	2090	2095	2100
SSP1	million	23,391	25,630	27,857	30,022	31,969	33,765	35,306	36,575	37,606	38,440	39,081	39,528	39,760	39,767	39,557	39,128	38,486	37,642	36,623
SSP2	million	23,391	25,991	28,638	31,263	33,801	36,212	38,469	40,492	42,293	43,911	45,387	46,690	47,774	48,672	49,385	49,881	50,161	50,245	50,194
SSP3	million	23,391	26,099	28,973	31,997	35,199	38,253	41,194	44,032	46,765	49,460	52,006	54,292	56,515	58,553	60,527	62,390	64,126	65,782	67,369
SSP4	million	23,391	26,098	28,970	31,980	35,150	38,157	41,044	43,827	46,500	49,126	51,593	53,805	55,960	57,938	59,853	61,655	63,327	64,912	66,421
SSP5	million	23,391	25,625	27,839	29,974	31,875	33,615	35,092	36,293	37,254	38,015	38,582	38,969	39,152	39,123	38,888	38,446	37,802	36,965	35,960

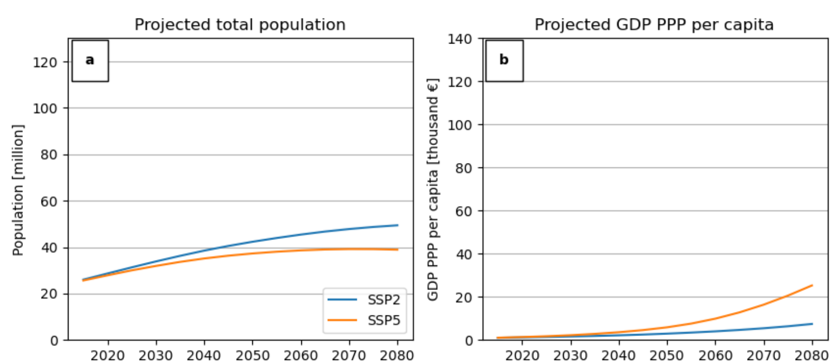

Figure S2 Population growth (a) and GDP PPP growth (b) over time for Mozambique based on IIASA

S1.4 Initiate attributes for coastal households

Socio-economic characteristics: Ton, Marijn, (2023) provide characteristics of people and households in a global agent database and wealth classes for households. We use the mean income and the ratio of wealth to income for Mozambique to estimate absolute household wealth. In addition, we classify households living in the coastal zone using the floodplain projected for 2080 by Ward et al. (2020) for a 1/100-year return period under the RCP8.5 scenario.

Farm size allocation: Lowder et al. (2016) provide the distribution of farm size under ranges of farm size in hectares (for ranges and distribution per country, see Annex 2 in S1.2). We use a log-normal distribution to generate absolute farm sizes and allocate them to farming households, assuming that the farm area owned by the farming household is directly proportional to its wealth.

Soil salinity map: We use the latest available global soil salinity map from Hassani et al. (2020) as our base map in 2015 and project it for different SLR scenarios discussed in the Methods section. The maps produced by Hassani et al. (2020) are quite detailed, but for missing data values in the floodplain, we adjust the data by performing a bilinear interpolation. There is also a dynamic map that runs within the model and is updated every year based on two physical processes: SLR and storm surge. Based on individual locations and this dynamic map, households experience soil salinity on their farms.

Crop type: GAEZ provides harvested area per crop per unit area (100 km^2). We first downscale these land use maps using the nearest resampling approach and then use the harvested area as a proxy for the probability of cultivating a particular crop to assign a crop type. For example, if a 1 km^2 area has 0.4 km^2 of rice, 0.3 km^2 of maize, 0.2 km^2 of cassava and 0.1 km^2 of sorghum, then a farming household is likely to cultivate a crop with a probability of [0.4, 0.3, 0.2, 0.1] for rice, maize, cassava and sorghum, respectively.

Household location: Household agents in the coastal flood zone are assigned locations based on the GHS 2015 population map (Schiavina, M. et al., 2019).

S1.5 Coastal population projection

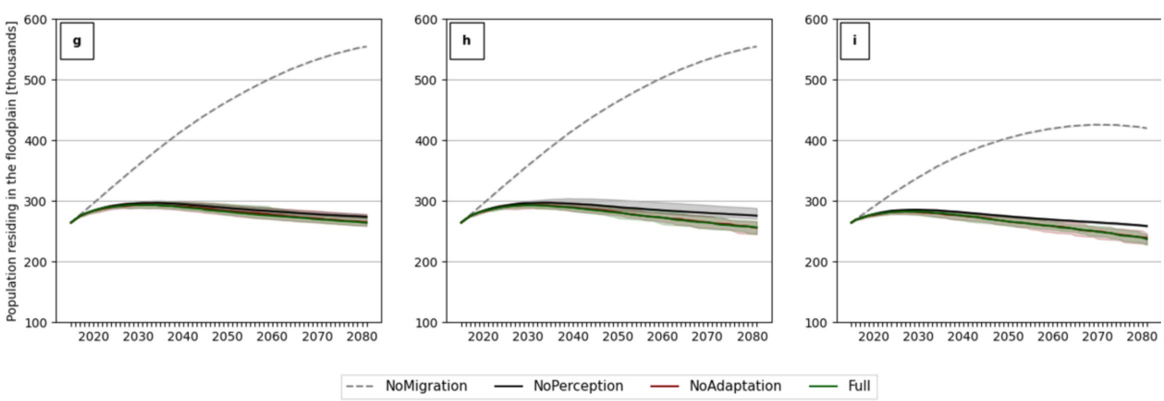

Figure S3 Coastal population under different RCP-SSP and behaviour scenarios.

S1.6 Percentage adapted

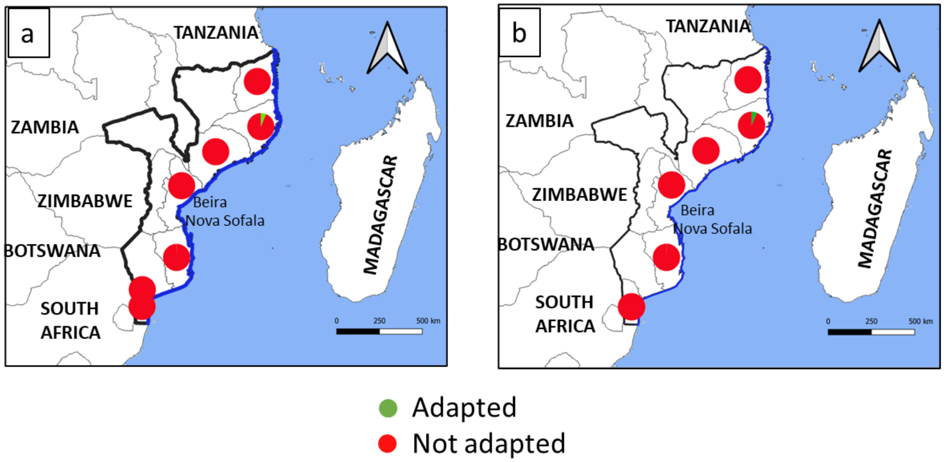

Figure S4 Percentage adapted under a) no perception and b) no adaptation setting.

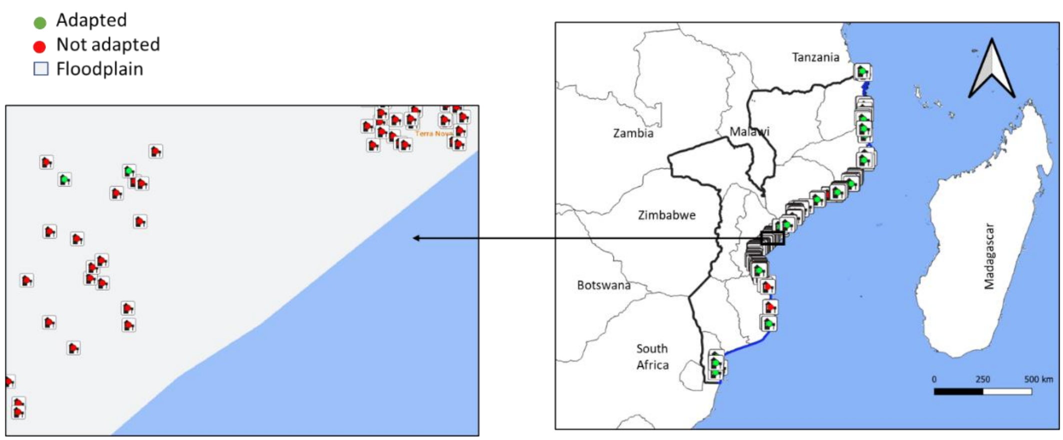

Figure S5 Number of farmers that have adapted or not adapted to salinity and flood risk in 2080 under increasing salt intrusion; left: individual households that have adapted; right: percentage of farmers that have adapted in each region.

S 2.1 Spin-up period

To start the model and simulate a situation in 2015, we ran the model for 15 periods, called “spin-up periods”. During this period, agents can make a decision to adapt or migrate, but no population growth or GDP growth rate is taken into account. These runs are made so that agents with the ability to adapt or migrate in 2015 can adapt or migrate and ensure that the results for the first year of our simulation (2016) are stable and not affected by sudden changes. After the spin-up period, it was found that about 9% of households in Sofala Province adapted, which is similar to the result based on the survey conducted by Sem J. Duijndam et al. (2023).

S 2.2 Coastal amenity function

Based on Conroy and Milosch, we construct a function to calculate the value of coastal amenities at a location in the floodplain as a function of distance to the coast (Figure S6). Household agents sample amenities based on their wealth and distance to the coast.

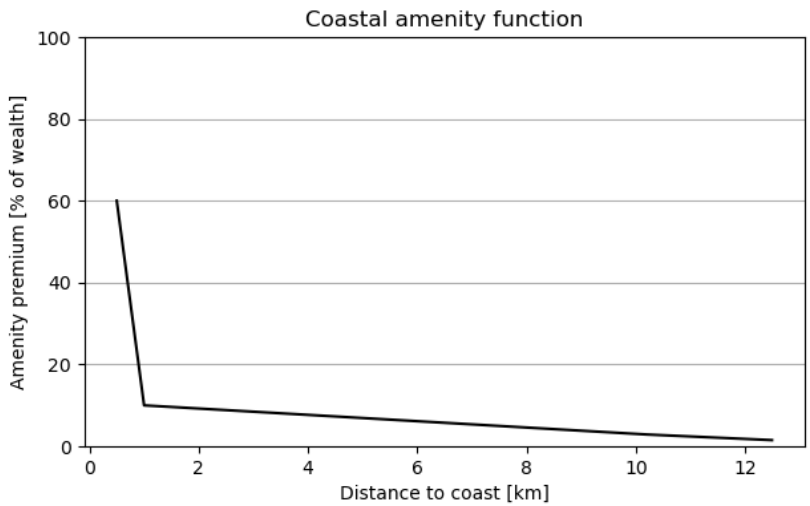

Figure S6 The coastal amenity function applied to determine the amenity value for a household in the floodplain.

Supplementary references

[1] Gao, F. & Han, L. Implementing the Nelder-Mead simplex algorithm with adaptive parameters. Comput. Optim. Appl. 2010 511 51, 259–277 (2010).

[2] de Ruig, L.T., Haer, T., de Moel, H. et al. How the USA can benefit from risk-based premiums combined with flood protection. Nat. Clim. Chang. 12, 995–998 (2022). https://doi.org/10.1038/s41558-022-01501-7

[3] Fischer, G., Nachtergaele, F. O., van Velthuizen, H., Chiozza, F., Francheschini, G., Henry, M., ... & Tramberend, S. (2021). Global agro-ecological zones (gaez v4)-model documentation.

[4] Gandelman, Nestor and Hernandez-Murillo, Ruben, Risk Aversion at the Country Level (2015). Available at SSRN: https://ssrn.com/abstract=2646134

[5] Schiavina, M., Freire, S. & MacManus, K. GHS population grid multitemporal (1975, 1990, 2000, 2015) European Commission, Joint Research Centre (JRC). (2019).

[6] Schiavina, M., Freire, S. & MacManus, K. GHS population grid multitemporal (1975, 1990, 2000, 2015) European Commission, Joint Research Centre (JRC). (2019).

[7] Ton, Marijn, 2023, "GLOPOP-S", https://doi.org/10.7910/DVN/KJC3RH, Harvard Dataverse, V3

[8] United Nations. World Population Prospects - Population Division - United Nations. https://population.un.org/wpp/Download/Archive/Standard/ (2019).

[9] Ward, P. J., Winsemius, H. C., Kuzma, S., Bierkens, M. F. P. P., Bouwman, A., Moel, H. D., Loaiza, A. D., Eilander, D., Englhardt, J., Gilles, E., Gebremedhin, E. T., Iceland, C., Kooi, H., Ligtvoet, W., Muis, S., Scussolini, P., Sutanudjaja, E. H., Beek, R. V., Bemmel, B. V., … Luo, T. (2020). Aqueduct Floods Methodology. In World Resources Institute (January; pp. 1–28). https://www.wri.org/research/aqueduct-floods-methodology www.wri.org/publication/aqueduct-floods-methodology